GEOPHYSICAL RESEARCH LETTERS, VOL. 33, L17714, doi:10.1029/2006GL027086, 2006

Assessment of composite global sampling: Sea surface wind speed

Huai-Min Zhang,[1] John J. Bates,[1] and Richard W. Reynolds[1]

Received 5 June 2006; revised 20 July 2006; accepted 10 August 2006; published 14 September 2006.

[1] Research and forecasts of the weather-ocean-climate system demand increasingly higher resolution forcing data. Here we assess the improvement in composite global observations and the feasibility of producing high resolution blended sea winds. The number of the long-term US sea surface wind speed observing satellites has increased from one in July 1987 to five or more since 2000. Global 0.25° gridded, blended products with temporal resolutions of 6-hours, 12-hours and daily have become feasible since mid 2002, mid 1995 and January 1991, respectively (with ≥75% time coverage and ≥90% spatial coverage between 65°S–65°N). If the coverage is relaxed, the feasible times can be extended to earlier periods. These statistics provide practical guidance to produce reliable blended products for different applications, and serve as guidance on the design of future global observing systems. **Citation:** Zhang, H.-M., J. J. Bates, and R. W. Reynolds (2006), Assessment of composite global sampling: Sea surface wind speed, *Geophys. Res. Lett.*, *33*, L17714, doi:10.1029/2006GL027086.

1. Introduction

[2] The Earth's weather and climate system is driven by two major constantly changing components – the atmosphere and the ocean. These two components vigorously interact with each other over about 70% of the Earth's surface and these interactions directly regulate the Earth's water and energy cycles. Advances in understanding this coupled system and improvements in numerical weather and ocean forecasts demand increasingly higher resolution data on wind and air-sea fluxes, as documented in several World Meteorological Organization (WMO) programs [e.g., *World Meteorological Organization*, 2000; *Curry et al.*, 2004] [also *Large et al.*, 1991]. Some of the applications require temporal and spatial resolutions of up to 3 hours and 50 km. However, to what extent these requirements can be met in reality by the existing global observing system of multiple satellites and in-situ observations has not been systematically studied. In this work we seek to answer this question for sea wind speed, a dominant parameter in forcing numerical models and in determining the turbulent air-sea fluxes [e.g., *Fairall et al.*, 2003].

[3] The composite statistics will be presented in the following sections with increasing complexity, and the results and discussion of one section will serve as the foundation for the next section. Section 2 describes the available sea wind observations. Section 3 presents a case study of the composite sampling in a day. Section 4 extends the composite analysis to the whole sea-wind satellite era in terms of averaged sampling time intervals. Section 5 examines the spatial and temporal data coverage for specific temporal resolutions. Lastly, section 6 features the summary and discussion.

2. Sea Surface Wind Speed Observations

[4] Sea surface wind has been traditionally observed from in-situ platforms such as ships and buoys [e.g., *Bourassa et al.*, 2005; *Worley et al.*, 2005]. However, even today in-situ observations still have very limited spatial coverage over the vast ocean surface. Sea surface wind speed has also been operationally observed from satellite sensors, starting with a US Defense Meteorological Satellite Program (DMSP) satellite F08 in July 1987 to the constellation of 5 or more US satellites since 2000. In this satellite era, in-situ observations still play a critical role in calibrating and validating satellite observations. However, with the dense satellite sampling, in-situ observations play a minor role in reducing random and sampling errors in blended analyses using in-situ and satellite observations [e.g., *Zhang et al.*, 2006]. Thus in this data sampling study, we only consider satellite observations.

[5] The time line of the long-term US sea surface wind speed observing satellites is shown in Figure 1. Note that in this long-term assessment study, we have not used the short-lived wind satellites (e.g., the US National Aeronautics and Space Agency Scatterometer (NSCAT), the joint US/Japan SeaWinds on the Advanced Earth Observing Satellites (ADEOS) I & II), non-US satellites (e.g., the European Remote Sensing Satellites (ERS) −1 and 2, which have narrow observing swaths and interrupted observations), and satellites from which sea surface wind speed can also be retrieved (presently with less accuracy) along with the primary product of sea level (e.g., the joint US/French altimetry satellites of Ocean Topography Experiment (TOPEX)/Poseidon and the follow-on Jason). Inclusion of these data would have limited positive impact for the corresponding time periods on this sampling study.

[6] Among the satellites in Figure 1, the passive DMSP observations are from the microwave radiometers on the Special Sensor Microwave Imager (SSMI [*Hollinger et al.*, 1987; *Wentz*, 1997]). Later additions to these passive microwave observations are the Tropical Rainfall Measuring Mission (TRMM) Microwave Imager (TMI [*Kummerow et al.*, 1998]) and the Advanced Microwave Scanning Radiometer of NASA's Earth Observing System (AMSR-E [e.g., *Wentz and Meissner*, 1999]). The scatterometer (e.g., the Quick Scatterometer (QuikSCAT)), which is active by nature, uses microwave radar and retrieves both wind speed and wind direction [e.g., *Dunbar et al.*, 1991a, 1991b; *Liu et al.*, 1998].

[1]National Climatic Data Center, NOAA NESDIS, Asheville, North Carolina, USA.

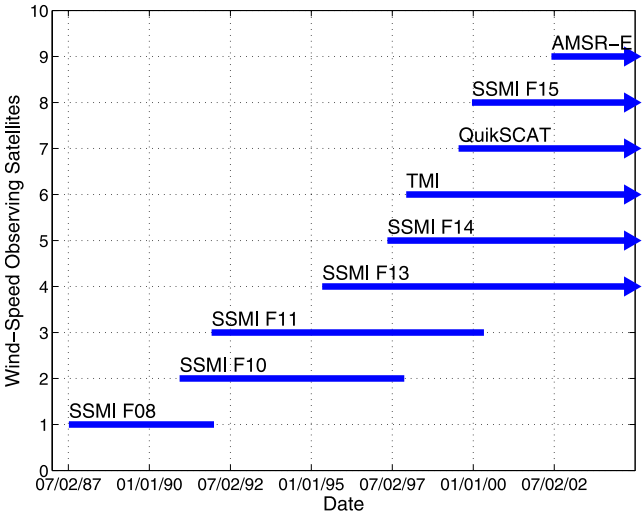

Figure 1. Timeline of the long-term US sea surface wind speed satellites used in this study.

[7] In the following we quantify the temporal improvement of the composite global data sampling rate from the satellites shown in Figure 1. The individual satellite data were obtained from the Remote Sensing Systems (RSS), Inc. [e.g., *Wentz*, 1997]. The RSS data were chosen for their uniformity of the retrieval algorithms for the multiple satellites over the whole time period, and for their wide use in producing various air-sea turbulent fluxes [e.g., *Chou et al.*, 2003, and references therein]. Using these datasets, we explore the possibility of producing blended global products on a 0.25° global grid for various temporal resolutions. This 0.25° spatial grid marginally resolves ocean boundary currents such as the Gulf Stream where large turbulent fluxes and large flux gradients frequently occur. An improved daily sea surface temperature analysis is also produced on this spatial grid [*Reynolds et al.*, 2006].

3. Daily Composite Global Sampling: A Case Study

[8] This section describes a case study to lay out the fundamental satellite observational information for the statistical analyses in the following sections. Figure 2 shows an example of the composite observations from the six satellites since mid 2002. The equator-crossing-times (ECTs) in Local Solar Time (LST) of the five polar-orbiting satellites (DMSP F13, F14, F15, QuikSCAT and AMSR-E) are typical for this time period, and the actual observation times in LST along individual tracks from the Equator to mid latitudes vary little, but change more rapidly in the Polar Regions (thus shown as long lines but not drawn near the Pole). In contrast, the ECTs of the equator-orbiting TMI satellite vary from day to day (shown for January 20) and the actual observation times also vary more rapidly even along a single track between roughly 40°N and 40°S (thus shown by short lines). Overall, the shown satellites are not evenly positioned around the Earth; however, with all the ascending and descending tracks, the observations span over the whole day fairly well with the additions of the TMI and AMSR-E.

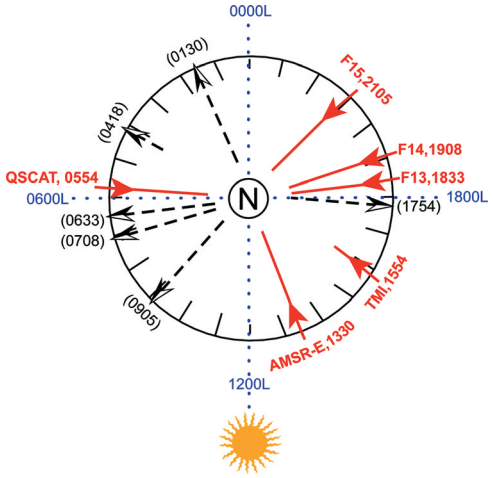

Figure 2. A simplified view looking down at the North Pole of the satellite observations in Local Solar Time (LST) of January 2005. Solid lines and arrows indicate ascending tracks and dashed lines and open arrows indicate descending tracks.

[9] The above is a quasi-Lagrangian view following the satellite tracks in local solar time. However, most gridded global products are generated as Eulerian fields on Earth, i.e. as global snapshots at specific Coordinated Universal Time (UTC) or as averages over certain UTC time periods. The Eulerian fields are required by many applications such as numerical modeling and computation of wind stress divergence or vorticity (when used together with wind directions). Figure 3 shows the distribution of the combined

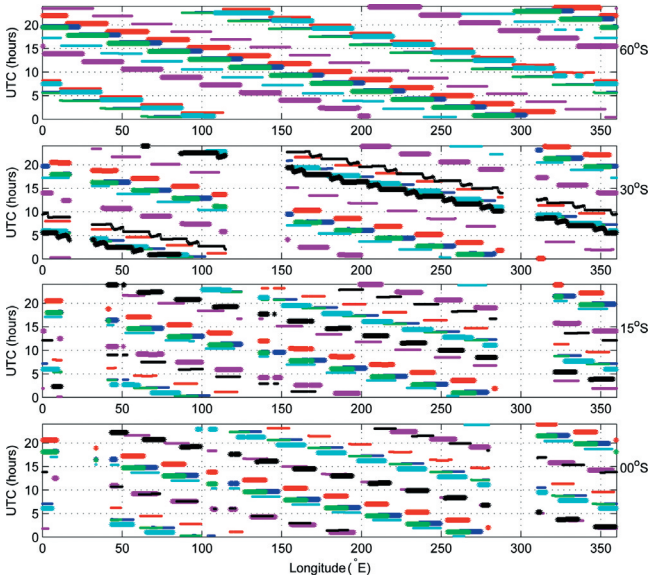

Figure 3. Oceanic satellite passing time (in UTC) along four latitude circles for 1 January 2005. Data bins are 0.25° by 0.25° in space. Top to bottom panels are for 60°S, 30°S, 15°S and the Equator, respectively. Thicker lines by '+' signs indicate ascending tracks and thinner lines by '.' signs indicate descending tracks. Each color represents one satellite: Red – F15, blue – F14, green – F13, black – TMI, cyan – QuikSCAT, and magenta – AMSR-E.

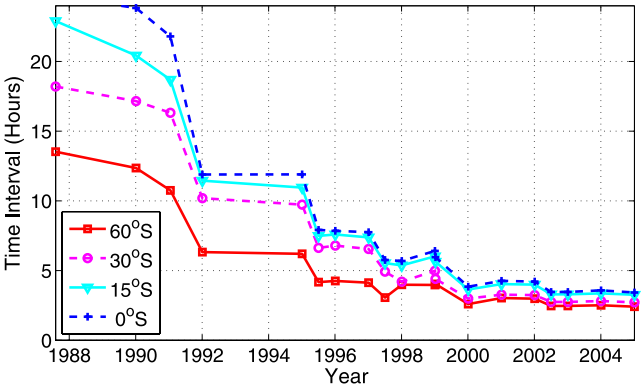

Figure 4. Averaged sampling time interval in the 0.25° bins, as functions of time and selected latitudes. Shown are averages along the individual latitude circles and over 1-week periods at the beginning of selected months, for which there were new satellite additions or reductions.

satellite observation times in UTC as functions of longitude (x-axis) and latitude (top to bottom panels). Sampling features in the Northern Hemisphere are similar but with more land masses (shown as horizontal data gaps).

[10] On this date (1 January 2005) and in most areas of the global ocean, the 0.25° bins are sampled multiple times (about 9.9, 8.7, 7.3 and 6.9 times on zonal average at the four latitudes) and the sampling times spread out over the 24-hour period fairly well although there are not strictly uniform. The slanting structure reflects the paths of the polar-orbiting satellites which result in a general sampling increase with increasing latitude.

4. Temporal Improvement in Averaged Sampling Time Intervals

[11] From Figure 3 and at fixed longitude and latitude, differencing the adjacent observing times results in individual sampling time intervals:

$$\Delta t_i = t_{i+1} - t_i,$$

where i indicates the discrete time points. The sampling time intervals are general not uniform in neither time nor space (Figure 3); here we first present an averaged view in Figure 4 (more detailed studies in sections to follow). The averaged sampling time intervals generally decreased with increasing latitudes (shown by the four curves). They also decreased rapidly from late 1987 to mid 1990s, from more than 14 hours to less than 8 hours. Further decreases from the mid 1990s were more moderate and the tropics and high latitudes eventually converged in early 2000, at which the averaged time intervals decreased to less than 5 hours.

[12] The averaged views are only useful for relatively uniform spacing of the data points (e.g., Figure 3). For highly inhomogeneous data distribution (in either time or space), the conclusion from this type of averaging may be misleading, as easily seen from the formulation of the time averaging:

$$\overline{\Delta t} = \frac{\Delta t_1 + \Delta t_2 + \ldots + \Delta t_{N-1}}{N-1} = \frac{t_N - t_1}{N-1},$$

where the bar indicates the average between time t_N and t_1. The above average depends only on the two end points and the total number of the observations, N. It does not depend on how the data are distributed between the end points. A worst hypothetical scenario would be that the six satellites observe at the same time. In this case the actual sampling resolution is more like $t_N - t_1$ rather than the averaged sampling time interval $(t_N - t_1)/(N-1)$. Some other cases for the scatterometer satellites have been discussed by *Schlax et al.* [2001].

5. Data Coverage for Various Fixed Resolutions

[13] In this section we present detailed assessment of the more realistic data coverage for the global 0.25° grid and various temporal resolutions (6-hourly, 12-hourly and daily) over the whole wind-satellite era. The first shown will be the temporal percentage data coverage for fixed spatial and temporal resolutions. Specifically, for each 0.25° grid box and fixed temporal resolution (i.e., sampling time interval, e.g., 6 hours), the percentage in time with data coverage over a month was computed, as shown in Figure 5 for January 2005. This picture is typical for the time period since mid 2002 when the AMSR-E was added. In the mid latitudes (40°S–60°S and 40°N–60°N), the vast majority of the global 0.25° boxes are sampled nearly 100% of the time within each 6-hour time window. The majority of the 0.25° boxes in the low to mid latitudes (40°S–40°N) are also sampled more than 75% of the time. Overall, about 92% of the global 0.25° oceanic boxes between 65°S–65°N are sampled 75% of the time or better within each 6-hour time period.

[14] Different applications (e.g., studies on cyclones, coastal ocean forecast, and global modeling) may have different requirements on data coverage. The above temporal and spatial data coverage statistics were also computed for other time periods and for the temporal resolutions of 6-hourly, 12-hourly and daily. The results are listed in Table 1 and will be summarized in the next section. In this table, the

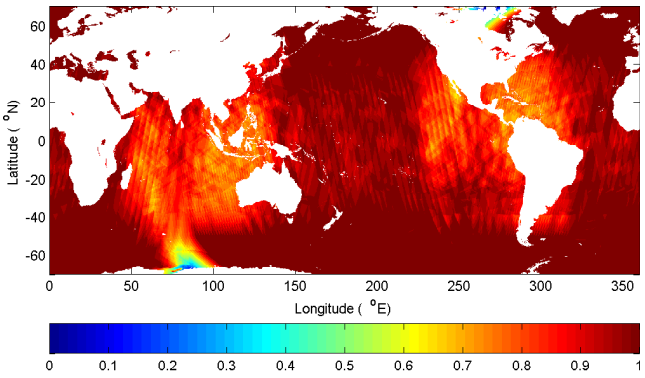

Figure 5. Temporal percentage of data availability within a month (January 2005) for a time interval of 6-hours (03Z – 09Z) and on the global 0.25° grid. Color scale 1 indicates data availability of 100% of the time.

Table 1. Typical Percentages of the Global 0.25° Oceanic Boxes Between 65°S and 65°N In Which There Are Data Coverage 75% of the Time or Better for the Specified Time Resolutions and as Functions of Time[a]

	Time Period and Satellite					
Time Resolution	JUL1987, I F08	JAN1991, II F10, F11	JUN1995, III F10, F11, F13	JAN1998, IV F11, F13, F14 TMI	JAN2000, V F13, F14, F15 TMI, QSCAT	JUN2002, VI F13, F14, F15 TMI, QSCAT AMSR-E
6-hourly	12	26	42	56	66	**91**
12-hourly	27	72	**97**	**99**	**100**	**100**
Daily	75	**100**	**100**	**100**	**100**	**100**

[a]The whole time period is classified into six stages corresponding to the typical number of available satellites. The time periods with ≥90% spatial coverage and ≥75% temporal coverage are bold.

sea-wind satellite era is classified into six time periods according to the number of available satellites and the resulting data coverage improvements. The listed spatial percentage coverage is for temporal percentage coverage of ≥75% for each 0.25° grid box.

6. Summary and Discussion

[15] Research and forecasts of the weather-ocean-climate system demand increasingly higher resolution forcing data. In this paper, we assessed the feasibility of producing various high resolution blended products for sea surface wind speed from the existing global observing system.

[16] At the temporal resolution of daily (24 hours, bottom row in Table 1), one SSMI satellite in stage I provided data coverage over about 75% of the global 0.25° oceanic boxes between 65°S–65°N. Beginning with stage II when there were two or more satellites, the spatial coverage was increased to about 100%.

[17] At the temporal resolution of 12-hourly (2nd row from the bottom in Table 1), one satellite in stage I provided data coverage to less than 30% of the oceanic grid boxes. The addition of the second SSMI satellite in stage II drastically increased the spatial coverage to just below 75%. Beginning with stage III when there were three or more satellites, the spatial coverage was increased to above 95%.

[18] At the temporal resolution of 6-hourly (3rd row from the bottom in Table 1), the spatial coverage was less than 30% with two or fewer satellites in stages I and II. In stage III, the coverage was about 42% with the three SSMI satellites (F10, F11 and F13). In stage IV, with the addition of the TMI, the spatial coverage increased to about 56%. In stage V, the addition of the QuikSCAT further increased the spatial coverage to about 66%. This modest increase is due to the close sampling times of the QuikSCAT and the SSMI satellites (Figure 2), although their ascending and descending tracks are out-of-phase. However, in stage VI, the addition of the AMSR-E dramatically increased the spatial coverage to above 90%. The critical importance of the AMSR-E for high resolution products (6-hourly in this case) was also previously indicated by its unique sampling times compared to the other satellites (Figure 2).

[19] In conclusion, on the global 0.25° grid, blended products with temporal resolutions of 6-hours, 12-hours and daily have become feasible since mid 2002, mid 1995 and January 1991, respectively (with ≥75% time coverage and ≥90% spatial coverage between 65°S–65°N). The corresponding feasible times can be farther extended back to the beginning of 2000, beginning of 1991 and late 1987 when the minimum spatial coverage was reduced to 65%, 70% and 75%, respectively for the above three temporal resolutions.

[20] Lastly, we mention our available blended sea surface wind speed product. This product is based on the above statistics and for an initially uniform blending for the whole sea wind satellite era (July 1987 – present), thus a 12-hourly time window was chosen. Sub-sampling aliases may still be large in this product for the early few years (Table 1). To take the advantage of the denser sampling in the latter years (especially since mid 2002), the blended data were generated 4 times a day at 00, 06, 12 and 18Z. To avoid heavy smoothing for the latter years with dense data, a Gaussian-like weighting function in both time and space was used to "penalize" data farther away from the interpolation points [*Zeng and Levy*, 1995]. The gridded data and data production details are available at http://www.ncdc.noaa.gov/oa/rsad/blendedseawinds.html. Validation by in-situ data, data error analysis and intercomparisons with other products are subjects of future investigation.

[21] **Acknowledgments.** The individual satellite data were downloaded from the website of the Remote Sensing System, Inc. (http://www.remss.com/). We thank Debra Smith (Remote Sensing System) for answering our detailed questions. Suggestions and critical comments from Ken Knapp and Lei Shi were a great help. Stimulating comments from two reviewers on an early version are greatly appreciated and enhanced the presentation. The views and findings in this report are those of the authors and should not be construed as an official NOAA or U.S. Government position, policy or decision.

References

Bourassa, M. A., R. Romero, S. R. Smith, and J. J. O'Brien (2005), A new FSU winds climatology, *J. Clim.*, *18*, 3692–3704.

Chou, S. H., E. Nelkin, J. Ardizzone, R. M. Atlas, and C. L. Shie (2003), Surface turbulent heat and momentum fluxes over global oceans based on the Goddard satellite retrievals, version 2 (GSSTF2), *J. Clim.*, *16*, 3256–3273.

Curry, J. A., et al. (2004), SEAFLUX, *Bull. Am. Meteorol. Soc.*, *85*(3), 409–424.

Dunbar, R. S., S. V. Hsiao, and B. H. Lambrigtsen (1991a), Science algorithm specifications for the NASA Scatterometer Project: Sensor Algorithms, *JPL D-5610-1*, Jet Propul. Lab., Pasadena, Calif.

Dunbar, R. S., S. V. Hsiao, and B. H. Lambrigtsen (1991b), Science algorithm specifications for the NASA Scatterometer Project: Geophysical Algorithms, *JPL D-5610-2*, Jet Propul. Lab., Pasadena, Calif.

Fairall, C. W., E. F. Bradley, J. E. Hare, A. A. Grachev, and J. B. Edson (2003), Bulk parameterization of air–sea fluxes: Updates and verification for the COARE algorithm, *J. Clim.*, *16*, 571–591.

Hollinger, J., R. Lo, G. Poe, R. Savage, and J. Pierce (1987), Special Sensor Microwave/Imager's user's guide, technical report, 120 pp., Nav. Res. Lab., Washington, D. C.

Kummerow, C., W. Barnes, T. Kozu, J. Shiue, and J. Simpson (1998), The Tropical Rainfall Measuring Mission (TRMM) sensor package, *J. Atmos. Oceanic Technol.*, *15*, 809–817.

Large, W. G., W. R. Holland, and J. C. Evans (1991), Quasi-geostrophic response to real wind forcing: The effects of temporal smoothing, *J. Phys. Oceanogr.*, *21*, 998–1017.

Liu, W. T., W. Tang, and P. S. Polito (1998), NASA scatterometer provides global ocean-surface wind fields with more structures than numerical weather prediction, *Geophys. Res. Lett.*, *25*(6), 761–764.

Reynolds, R. W., K. S. Casey, T. M. Smith, D. B. Chelton (2006), A daily blended analysis for sea surface temperature, paper presented at 86th AMS Annual Meeting, Am. Meteorol. Soc., Boston, Mass.

Schlax, M. G., D. B. Chelton, and M. H. Freilich (2001), Sampling errors in wind fields constructed from single and tandem scatterometer datasets, *J. Atmos. Oceanic Technol.*, *18*, 1014–1036.

Wentz, F. J. (1997), A well-calibrated ocean algorithm for SSM/I, *J. Geophys. Res.*, *102*(C4), 8703–8718.

Wentz, F. J., and T. Meissner (1999), AMSR Ocean Algorithm, version 2, *Tech. Rep. 121599a*, Remote Sens. Syst., Santa Rosa, Calif.

World Meteorological Organization (2000), Final report of the Joint WCRP/SCOR Working Group on Air-Sea Fluxes (SCOR Working Group 110): Intercomparison and validation of ocean-atmosphere energy flux fields, *WMO/TD-1036/WCRP-112*, 303 pp., Geneva.

Worley, S. J., S. D. Woodruff, R. W. Reynolds, S. J. Lubker, and N. Lott (2005), ICOADS release 2.1 data and products, *Int. J. Climatol.*, *25*, 823–842.

Zeng, L., and G. Levy (1995), Space and time aliasing structure in monthly mean polar orbiting satellite data, *J. Geophys. Res.*, *100*(D3), 5133–5142.

Zhang, H.-M., R. W. Reynolds, and T. M. Smith (2006), Adequacy of the in situ observing system in the satellite era for climate SST, *J. Atmos. Oceanic Technol.*, *23*, 107–120.

J. J. Bates, R. W. Reynolds, and H.-M. Zhang, National Climatic Data Center, NOAA NESDIS, 151 Patton Avenue, Asheville, NC 28801, USA. (huai-min.zhang@noaa.gov)